

Structure–Activity Relationship of Cyclic Nitroxides as SOD Mimics and Scavengers of Nitrogen Dioxide and Carbonate Radicals

Sara Goldstein,^{*,†} Amram Samuni,[‡] Kalman Hideg,[§] and Gabor Merenyi[#]

Department of Physical Chemistry, The Hebrew University of Jerusalem, Jerusalem 91904, Department of Molecular Biology, Hebrew University-Hadassah Medical School, P.O.B. 12000, Jerusalem 91120, Israel, Institute of Organic and Medicinal Chemistry, University of Pécs, H-7643 Pécs, Hungary, and Department of Chemistry, Nuclear Chemistry, The Royal Institute of Technology, S-10044 Stockholm 70, Sweden

Received: November 27, 2005; In Final Form: January 16, 2006

Synthetic nitroxide antioxidants attenuate oxidative damage in various experimental models. Their protective effect reportedly depends on ring size and ring substituents and is greater for nitroxides having lower oxidation potential. The present study focuses on the kinetics and mechanisms of the reactions of piperidine, pyrrolidine and oxazolidine nitroxides with $\text{HO}_2^*/\text{O}_2^{\bullet-}$, $\bullet\text{NO}_2$ and $\text{CO}_3^{\bullet-}$ radicals, which are key intermediates in many inflammatory and degenerative diseases. It is demonstrated that nitroxides are the most efficient scavengers of $\bullet\text{NO}_2$ at physiological pH ($k = (3-9) \times 10^8 \text{ M}^{-1} \text{ s}^{-1}$) and among the most effective metal-independent scavengers of $\text{CO}_3^{\bullet-}$ radicals ($k = (2-6) \times 10^8 \text{ M}^{-1} \text{ s}^{-1}$). Their reactivity toward HO_2^* , though not toward $\bullet\text{NO}_2$ and $\text{CO}_3^{\bullet-}$, depends on the nature of the ring side-chain and particularly on the ring-size. All nitroxide derivatives react slowly with $\text{O}_2^{\bullet-}$ and are relatively inefficient SOD mimics at physiological pH. Even piperidine nitroxides, having the highest SOD-like activity, demonstrate a catalytic activity of about 1000-fold lower than that of native SOD at pH 7.4. The present results do not indicate any correlation between the kinetics of $\text{HO}_2^*/\text{O}_2^{\bullet-}$, $\bullet\text{NO}_2$ and $\text{CO}_3^{\bullet-}$ removal by nitroxides and their protective activity against biological oxidative stress and emphasize the importance of target-oriented nitroxides, i.e., interaction between the biological target and specific nitroxides.

Introduction

Synthetic cyclic nitroxide radicals (RNO \bullet) persist in tissues and in the circulatory system^{1,2} primarily as the reduced form (RNO–H) and have been used as biophysical markers for monitoring membrane fluidity, cellular metabolism, intracellular pH or O_2 levels,^{3–6} and as potential contrast agents for magnetic resonance imaging^{7,8} and *in vivo* electron paramagnetic resonance imaging.⁹ Nitroxides attenuate oxidative damage in various experimental models, such as cultured cells,^{10,11} brain injury,^{12,13} lipid peroxidation in liver microsomes,¹⁴ thymocyte apoptosis,¹⁵ post-ischemic reperfusion injury in isolated organs^{16–18} and ionizing irradiation of rats and mice.^{19,20} Contrary to common nonenzymatic antioxidants, which are primarily reducing species, nitroxides can provide protection acting also as oxidants, e.g., through oxidation of reduced transition metals and, pre-empting their participation in the Fenton reaction,²¹ detoxification of semiquinones via their oxidation to quinones,²² and scavenging oxygen-, nitrogen- and carbon-centered radicals.^{23–30}

Recently, it has been reported that the electronic structure of the aminoxy moiety is unaffected by the ring substituents except in a carbonyl derivative and, therefore, electronic structure and electron delocalization play only a minor role in the reactions of nitroxides.³¹ Indeed, we have shown that the rate constants for the reactions of $\text{CO}_3^{\bullet-}$ or $\bullet\text{NO}_2$ with the five-membered ring 3-carbamoylproxyl are similar to those of the six-membered ring

2,2,6,6-tetramethylpiperidine-1-oxyl (TPO) and its derivatives 4-OH-TPO and 4-oxo-TPO.^{27,28,30} In contrast, we found that the rate constant of the reaction of HO_2^* with TPO is about 2 orders of magnitude higher than that with 3-carbamoylproxyl²⁹ and correlates well with the one-electron oxidation potential $E^\circ(\text{RN}^+=\text{O}/\text{RNO}^*)$ of the nitroxide.^{29,32} Furthermore, nitroxides with the lower oxidation potential exhibit greater protection against cellular damage by H_2O_2 or ionizing radiation.³³ The protective effect was not only dependent on the ring size but also on the ring substituents and charge.^{20,33} Nitroxides containing a basic side chain (e.g., 4-amino-TPO, 3-(aminomethyl)proxyl) provided a greater protection, whereas negatively charged nitroxides (e.g., 3-carboxyproxyl) provided minimum protection.^{20,33} The greater protective activity of 4-amino-TPO and 3-(aminomethyl)proxyl, which was not anticipated in view of their relatively high $E^\circ(\text{RN}^+=\text{O}/\text{RNO}^*)$, has been attributed to their greater affinity to negatively charged targets such as nucleic acids.^{20,33} The importance of target-oriented nitroxides has been previously demonstrated by the difference between the protective effects of H-2954, and its biologically inactive analogue TCPO (see Chart 1), for isolated cardiomyocytes against oxidative damage,³⁴ and the ability of Mito-carboxyproxyl, but not 3-carboxyproxyl, to protect the cells from peroxide-induced oxidative stress and apoptosis.³⁵

Yet, no clear mechanistic explanation for the observed dependence of the protective effect of nitroxides on their redox potential, ring substituent, or charge has previously been proposed. The present study focuses on the kinetics and mechanisms of the reactions of the nitroxide derivatives listed in Chart 1 with $\text{HO}_2^*/\text{O}_2^{\bullet-}$, $\bullet\text{NO}_2$ and $\text{CO}_3^{\bullet-}$ radicals, and emphasizes the importance of target-oriented nitroxides.

* To whom all correspondence should be directed. Tel. 972-2-6586478. Fax: 972-2-6586925. E-mail: sarag@vms.huji.ac.il.

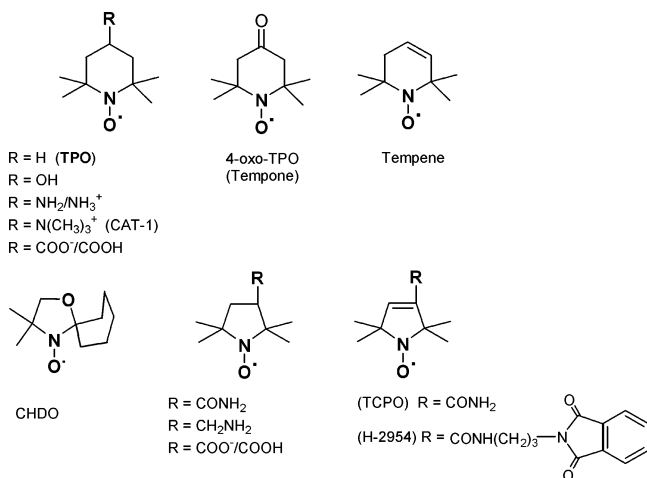
[†] The Hebrew University of Jerusalem.

[‡] Hebrew University-Hadassah Medical School.

[§] University of Pécs.

[#] The Royal Institute of Technology.

CHART 1



Experimental Section

Materials. All chemicals were of analytical grade and were used as received. Water for preparation of the solutions was purified using a Milli-Q purification system. TPO, 4-OH-TPO, 4-amino-TPO, 4-carboxy-TPO, 4-oxo-TPO (Tempone), 3-(aminomethyl)proxyl, 3-carboxyproxyl and 2-spiro-5,5-dimethyl-3-oxazolidine-1-oxyl (CHDO) were purchased from Aldrich. 4-trimethylammonium-TPO iodide (CAT-1) was a product of Molecular Probes Inc. Tempene, 2,2,5,5-tetramethyl-3-carbamido-3-pyrroline-1-oxyl (TCPO) and H-2954 were synthesized at the University of Pécs as previously reported.^{33,36,37} Stock solutions of 3-(aminomethyl)proxyl and H-2954 were prepared in CH₃CN, which reacts relatively slow with all the radicals formed by radiolysis.

Cyclic Voltammetry (CV). CV was performed with a BAS100B Electrochemical Analyzer. We used a three-electrode system consisting of a composite Ag/AgCl (3.5M NaCl) as a reference electrode, a platinum wire as an auxiliary electrode and ultra trace graphite (6-1204-100 Metrohm) as a working electrode. In a typical experiment, the electrodes were immersed in aqueous solution containing 4–100 mM phosphate buffer (PB) and 2–5 mM nitroxide at ambient temperature. The measured potentials were corrected for the potential of Ag/AgCl in 3.5 M NaCl, i.e., +205 mV, and quoted vs the normal hydrogen electrode (NHE).

Production of the Oxoammonium Cation (RN⁺=O). RN⁺=O was prepared by electrolysis of aerated solutions containing 200 μM RNO[•] and 4 mM PB using an electrochemical reactor. Briefly, the electrochemical cell consisted of a working electrode of graphite grains packed inside a porous Vycor glass tube (5 mm i.d.), through which the RNO[•] solution was pumped (2–5 mL min⁻¹). An outer glass cylinder, with separate electrolyte (10 mM PB, pH 7.0) contained the platinum auxiliary electrode. The voltage was controlled using a BAS100B Electrochemical Analyzer. The oxidation yield was determined spectrophotometrically using excess of either Fe(CN)₆⁴⁻ or 2,2'-azinobis(3-ethylbenzothiazoline-6-sulfonate) (ABTS²⁻), which were oxidized to Fe(CN)₆³⁻ (ε₄₂₀ = 1000 M⁻¹ cm⁻¹) or ABTS⁻ (ε₆₆₀ = 12000 M⁻¹ cm⁻¹), respectively.

Pulse Radiolysis. Pulse radiolysis experiments were carried out using a 5 MeV Varian 7715 linear accelerator (0.1–0.5 μs electron pulses, 200 mA current). A 200 W Xe lamp produced the analyzing light. Appropriate cutoff filters were used to minimize photochemistry. All measurements were made at room temperature in a 4 cm Spectrosil cell using three light passes

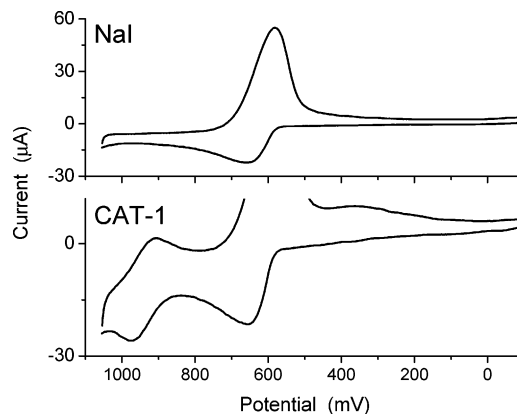


Figure 1. Cyclic voltammograms of 2 mM NaI and 2 mM CAT-1 in 100 mM PB at pH 2.0 measured at scan rate of 100 mV s⁻¹. Top: $E_{1/2} = 616$ mV for iodine/iodide couple. Bottom: $E_{1/2} = 611$ mV for iodide/iodine couple, $E_{1/2}^{\text{oxd}} = 942$ mV for the RN⁺=O/RNO[•] couple and the cathodic peak at 360 mV reflects the reduction of RNO[•] to RNO–H.

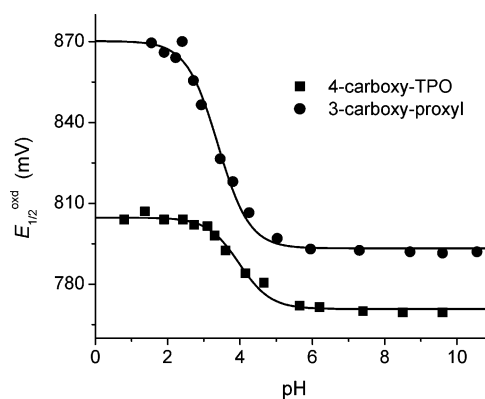


Figure 2. pH dependence of $E_{1/2}^{\text{oxd}}$ measured for 3–4 mM nitroxide in 4 mM PB. The solid line reflects the best sigmoidal fit to the experimental points. The plateau values represent $E_{1/2}^{\text{oxd}}$ for the protonated and deprotonated nitroxide. The midpoint of the sigmoidal functions reflects the pK_a of the nitroxide.

(optical path length 12.1 cm). The dose per pulse was determined with 5 mM KSCN in oxygenated solutions.³⁸

Results

CV. The results show a reversible one-electron redox reaction in the region of the positive potential attributable to the RN⁺=O⁺/RNO[•] couple. The reduction of RNO[•] to hydroxylamine (RNO–H) and its reoxidation show a pH-dependent irreversible wave as previously reported for TPO and 4-OH-TPO^{39,40} and will not be dealt with in the present paper. The CV of CAT-1 solutions, which contain equimolar concentrations of iodide could be determined only in acidic solutions where a single wave of iodide oxidation is observed, i.e., $E_{1/2} = 607 \pm 10$ mV. The latter value is well separated from that of the RN⁺=O/RNO[•] couple, i.e., $E_{1/2}^{\text{oxd}} = 940 \pm 5$ mV at pH 2–4 (Figure 1).

The $E_{1/2}^{\text{oxd}}$ for the carboxy-derivatives varied with the pH as demonstrated in Figure 2. The pK_a values obtained from the sigmoidal curves in Figure 2 are 3.4 and 4.0 for 3-carboxyproxyl and 4-carboxy-TPO, respectively, and are in agreement with previously reported values.^{41–43}

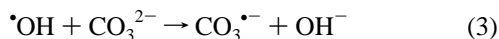
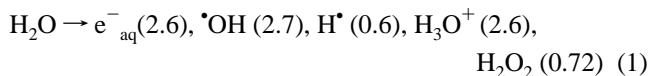
The $E_{1/2}^{\text{oxd}}$ of the protonated and deprotonated forms derived from the sigmoidal curves seen in Figure 2 are summarized in Table 1. One would expect to obtain a sigmoidal curve also for 4-amino-TPO (pK_a = 9.1 ± 0.1).⁴¹ However, the respective oxoammonium cation reacts extremely fast with 4-NH₂-TPO (results not shown), and therefore, a poorly defined anodic peak

TABLE 1: Oxidation Potential $E_{1/2}^{\text{oxd}}$ (mV) for the $\text{RN}^+=\text{O}/\text{RNO}^\bullet$ Couple

RNO [•]	this study	literature
TPO		740, ⁴⁰ 722, ³² 719, ⁴⁴ 732 ⁴⁵
4-COOH-TPO	805 ± 4	
4-COO ⁻ -TPO	770 ± 3	771 ⁴⁴
4-OH-TPO		825, ⁴⁰ 810, ³² 808, ⁴⁴ 720 ⁴⁶
4-NH ₃ ⁺ -TPO	892 ± 3 (pH 1.8–5.7)	826 (pH 7.4), ³² 872 (pH 7.2–0.4), ⁴⁶ 851 (pH 7.4) ⁴⁴
	817 (pH 7.4)	
4-N(CH ₃) ₃ ⁺ -TPO	940 ± 5	
4-oxo-TPO	918 ± 5	913, ³² 912 ⁴⁶
tempene	795 ± 4	
3-COOH-proxyl	870 ± 4	
3-COO ⁻ -proxyl	793 ± 3	792, ³² 772 ⁴⁶
3-CH ₂ NH ₃ ⁺ -proxyl		853 ³²
3-carbamoylproxyl		861, ³² 867, ⁴⁵ 872 ⁴⁶
TCPO	955 ± 5	
H-2954	1000 ± 6	
CHDO		900 ³²

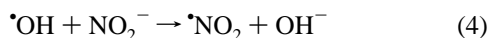
was observed at pH > 9, which disappeared at pH 11. The electrochemical behavior of 4-amino-TPO exhibited a reversible pH-independent wave for the $\text{RN}^+=\text{O}/\text{RNO}^\bullet$ redox couple at pH 1.8–5.7, implying $E_{1/2}^{\text{oxd}} = 892 \pm 3$ mV, which decreased somewhat upon increasing the pH, e.g., $E_{1/2}^{\text{oxd}} = 862$ and 817 mV at pH 6.8 and 7.4, respectively.

Reaction of RNO^\bullet with $\text{CO}_3^{\bullet-}$. The kinetics of the reaction of $\text{CO}_3^{\bullet-}$ with the nitroxides was studied upon pulse irradiation of N_2O -saturated solutions containing 0.1–0.5 M sodium carbonate at pH > 9. Under such conditions, e^-_{aq} and $\bullet\text{OH}$ formed by the radiation (eq 1) are converted into $\text{CO}_3^{\bullet-}$ through reactions 2 and 3. In eq 1 the values in parentheses are G values,



which represent the yields of the species (in 10^{-7} M Gy⁻¹). The decay of ca. 4 μM $\text{CO}_3^{\bullet-}$ was followed at 600 nm ($\epsilon_{600} = 1860$ M⁻¹ cm⁻¹) and turned from second-order into a fast first-order reaction in the presence of excess nitroxide, where k_{obs} increased linearly with increasing $[\text{RNO}^\bullet]_0$. In the case of 4-amino-TPO ($\text{p}K_{\text{a}} = 9.1$), the rate constant was independent of the pH in the pH-interval 9.1–11.7. Typical results are given in Figure 3. The bimolecular rate constants derived from such dependencies are summarized in Table 2.

Reaction of RNO^\bullet with $\bullet\text{NO}_2$. The kinetics of the reaction of $\bullet\text{NO}_2$ with excess nitroxide was studied indirectly upon pulse-irradiation of N_2O -saturated solutions containing 1–4 mM nitrite and 100 μM ABTS²⁻ at pH 3–10. Under such conditions, e^-_{aq} and $\bullet\text{OH}$ formed by the radiation (eq 1) are converted into $\bullet\text{NO}_2$ through reactions 2 and 4. As previously reported,²⁸ the



reaction of RNO^\bullet with $\bullet\text{NO}_2$ forms the respective oxoammonium cation, which is efficiently scavenged by ABTS²⁻ forming ABTS^{•-} ($\epsilon_{660} = 12000$ M⁻¹ cm⁻¹). The yield of ABTS^{•-} approached 100%, i.e., $[\bullet\text{NO}_2]_0 = [\text{ABTS}^{\bullet-}]$, independently of $[\text{RNO}^\bullet]_0$, whereas the rate of formation of ABTS^{•-} obeyed first-order kinetics and k_{obs} increased linearly with increasing $[\text{RNO}^\bullet]_0$. Typical results are given in Figure 3. The bimolecular rate constants derived from such dependencies are summarized in Table 2.

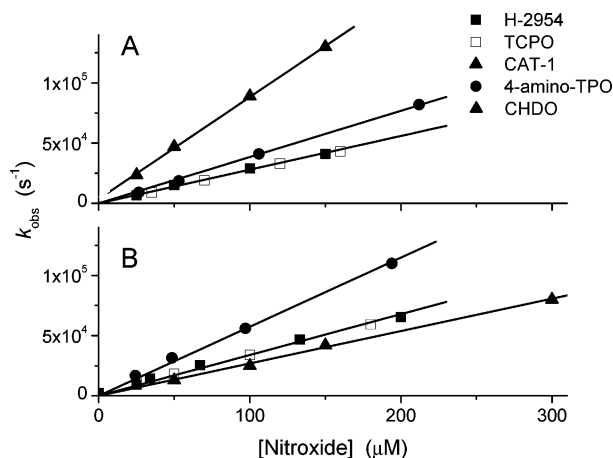


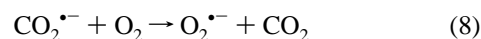
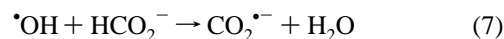
Figure 3. (A) Reaction of $\text{CO}_3^{\bullet-}$ with the nitroxides. The decay of $\text{CO}_3^{\bullet-}$ was followed at 600 nm upon pulse irradiation of N_2O -saturated solutions containing 0.1 M carbonate at pH 10.3. (B) Reaction of $\bullet\text{NO}_2$ with the nitroxides. The formation of ABTS^{•-} was followed at 660 nm upon pulse irradiation of N_2O -saturated solutions containing 2 mM nitrite, 100 μM ABTS²⁻ and 2.4 mM PB at pH 7.2.

TABLE 2: Rate Constants (M⁻¹ s⁻¹) Determined for the Reaction of RNO^\bullet with $\bullet\text{NO}_2$ and $\text{CO}_3^{\bullet-}$ Radicals^a

nitroxide	$\bullet\text{NO}_2$	$\text{CO}_3^{\bullet-}$
4-amino-TPO	$(5.5 \pm 0.2) \times 10^8$ (pH 3–10)	$(3.9 \pm 0.1) \times 10^8$ (pH 10.3)
CAT-1	$(4.0 \pm 0.1) \times 10^8$	$(6.3 \pm 0.1) \times 10^8$ ^b
3-carboxyproxyl	$(4.9 \pm 0.2) \times 10^8$ (pH 6.9)	$(2.4 \pm 0.1) \times 10^8$ (pH 10.1)
TCPO	$(3.2 \pm 0.1) \times 10^8$	$(2.7 \pm 0.1) \times 10^8$
H-2954	$(3.2 \pm 0.1) \times 10^8$	$(2.7 \pm 0.1) \times 10^8$
CHDO	$(2.5 \pm 0.1) \times 10^8$	$(2.6 \pm 0.1) \times 10^8$
TPO	$(7.1 \pm 0.2) \times 10^8$ ²⁸	$(4.0 \pm 0.1) \times 10^8$ ³⁰
4-OH-TPO	$(8.7 \pm 0.2) \times 10^8$ ²⁸	$(4.0 \pm 0.1) \times 10^8$ ¹⁸
4-oxo-TPO	$(7.1 \pm 0.2) \times 10^8$ ²⁸	$(4.0–4.8) \times 10^8$ ^{30,47}
3-carbamoylproxyl	$(7.1 \pm 0.2) \times 10^8$ ²⁸	$(4.0 \pm 0.1) \times 10^8$ ³⁰

^a The pH is given in cases where the nitroxide has a $\text{p}K_{\text{a}}$ in the studied pH range. ^b The value after correcting for $k(\text{CO}_3^{\bullet-} + \text{I}^-) = 2.5 \times 10^8$ M⁻¹ s⁻¹.⁴⁸

Reaction of RNO^\bullet with Superoxide. Superoxide radicals were generated upon irradiation of solutions saturated with O_2 and containing 5×10^{-3} to 2 M formate, 0–0.6 M phosphate and 5 μM diethylenetriaminepentaacetic acid (DTPA) to avoid metal-catalyzed superoxide dismutation. Under such conditions all radicals produced by the radiation (eq 1) are converted into superoxide ($\text{HO}_2^\bullet/\text{O}_2^{\bullet-}$, $\text{p}K_{\text{a}} = 4.8$)⁴⁹ via reactions 5–7. Both



HO_2^\bullet and $\text{O}_2^{\bullet-}$ have distinct absorption spectra in the UV region with maxima at 225 ($\epsilon = 1400$ M⁻¹ cm⁻¹) and 245 nm ($\epsilon = 2350$ M⁻¹ cm⁻¹), respectively.⁴⁹ The second-order decay of superoxide, observed at 270–290 nm turned into a first-order process in the presence of excess RNO^\bullet , and k_{obs} was linearly dependent on $[\text{RNO}^\bullet]_0$. However, the decay of superoxide could not be followed below 270 nm due to the absorption of RNO^\bullet . Therefore, at pH < 3.7 the reaction was studied indirectly in the presence of 100 or 200 μM ABTS²⁻, which efficiently scavenges $\text{RN}^+=\text{O}$ to form ABTS^{•-}, the latter reacting

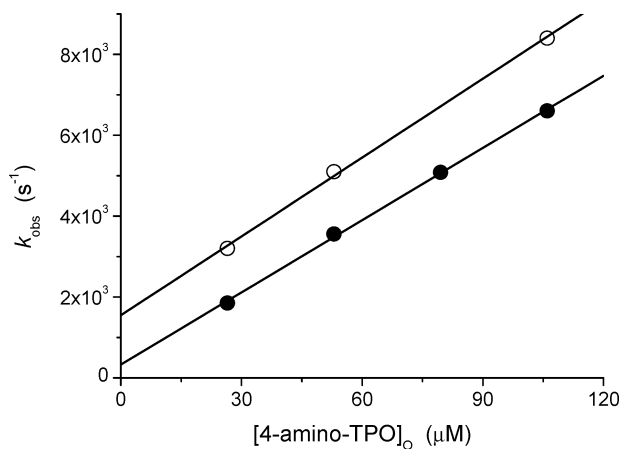


Figure 4. Reaction of superoxide with 4-amino-TPO at pH 3.7 in the absence and presence of 100 μM $\text{ABTS}^{\bullet-}$. The decay of superoxide was followed at 280 nm (empty circles) and that of the formation of $\text{ABTS}^{\bullet-}$ at 660 nm (solid circles) in oxygenated solutions containing 5 μM DTPA and 0.1 M formate.

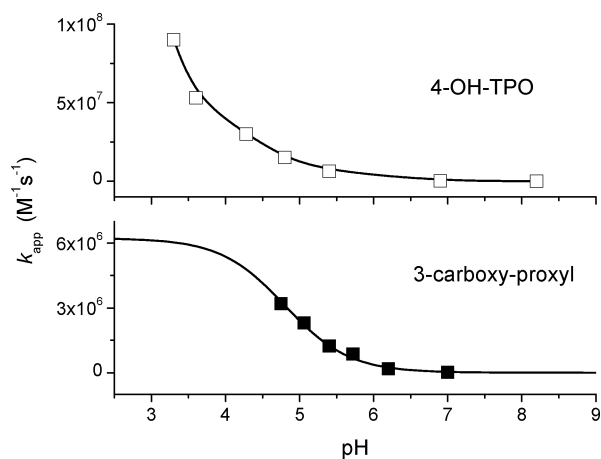


Figure 5. Apparent rate constant of superoxide reacting with 4-OH-TPO or 4-carboxyproxyl as a function of pH. All solutions contained 0–4 mM PB and 20 mM formate. In the case of 3-carboxyproxyl, the solid line reflects the best sigmoidal fit to the experimental points assuming $\text{p}K = 4.8$ and $k_{\text{app}} < 1 \times 10^4 \text{ M}^{-1} \text{ s}^{-1}$ for the lower asymptotic value.

extremely slowly, if at all, with HO_2^{\bullet} . The yield of $\text{ABTS}^{\bullet-}$ approached 100% ($[\text{superoxide}]_0 = [\text{ABTS}^{\bullet-}]$) independently of $[\text{RNO}^{\bullet}]_0$ and $[\text{ABTS}^{2-}]_0$. The formation of $\text{ABTS}^{\bullet-}$ obeyed first-order kinetics and k_{obs} increased with increasing $[\text{RNO}^{\bullet}]_0$, as demonstrated in Figure 4. Figure 4 also shows that the same bimolecular rate constant is obtained at pH 3.7, regardless of whether it is measured directly by following the decay of superoxide or indirectly by following the formation of $\text{ABTS}^{\bullet-}$.

As was shown in the cases of TPO and 3-carbamoylproxyl,²⁹ the rate constant of superoxide reaction with the nitroxides tested decreased with increasing pH, indicating that $\text{O}_2^{\bullet-}$ reacts with these nitroxides extremely slowly, e.g., Figure 5. However, in contrast to TPO,²⁹ the rate of superoxide reaction with all other six-membered ring nitroxides did not approach a plateau value below pH 3.7 (e.g., Figure 5), indicating that the reaction is acid-catalyzed.

The apparent rate constant, k_{app} , at a constant pH increased upon increasing the concentration of either formate (Figure 6) or phosphate (Figure 7), indicating that these buffers also catalyze the reaction.

The rate constant of superoxide reaction with 4-carboxy-TPO at pH 5.4 reached a plateau value of $(3.5 \pm 0.1) \times 10^7 \text{ M}^{-1} \text{ s}^{-1}$

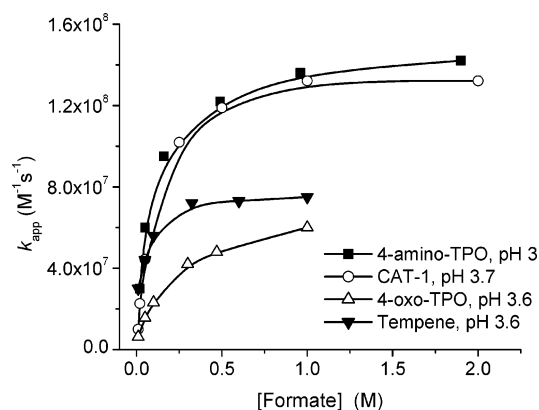


Figure 6. Effect of formate concentration on the rate of superoxide reaction with TPO derivatives. The formation of $\text{ABTS}^{\bullet-}$ in oxygenated solutions containing 5 μM DTPA, 100 μM ABTS^{2-} and formate was followed. k_{app} was obtained from the dependence of k_{obs} on $[\text{RNO}^{\bullet}]$ at constant [formate].

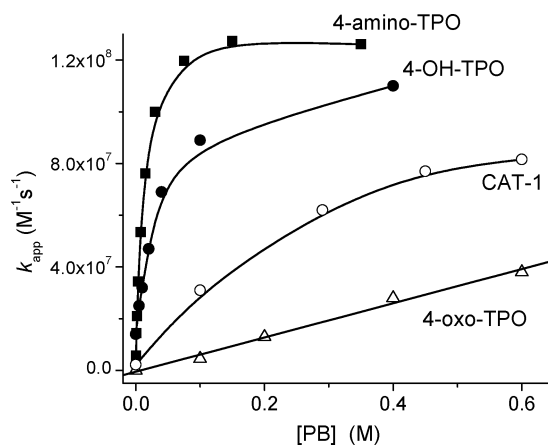


Figure 7. Effect of phosphate concentration on the rate of superoxide reaction with TPO derivatives. The decay of superoxide in oxygenated solutions containing 5 μM DTPA, 5 mM formate and PB at pH 4.8 was followed. k_{app} was obtained from the dependence of k_{obs} on $[\text{RNO}^{\bullet}]$ at constant [PB].

at $[\text{PB}] > 0.3 \text{ M}$. The apparent bimolecular rate constants of HO_2^{\bullet} reaction with the neutral 4-carboxy-TPO were determined to be $(1.1 \pm 0.1) \times 10^8$ and $(1.4 \pm 0.1) \times 10^8 \text{ M}^{-1} \text{ s}^{-1}$ at pH 3.0 and 2.4, respectively. Iodide reacts extremely slowly, if at all, with HO_2^{\bullet} , and therefore, its presence in CAT-1 solutions could be ignored.

As in the case of 3-carbamoylproxyl, the rate of superoxide reaction with all five-membered ring nitroxides was hardly affected upon increasing the concentration of phosphate up to 0.6 M at pH 4.8 and was slightly affected by decreasing the pH from 3.6 to 2.7 (Table 3). Because the $\text{p}K_{\text{a}}$ of 3-carboxyproxyl is 3.4, the reaction of superoxide with the deprotonated form was studied at $\text{pH} > 4.7$. The apparent bimolecular rate constant decreased with increasing pH, and an excellent sigmoidal fit was obtained by use of $\text{p}K_{\text{a}}(\text{HO}_2^{\bullet}) = 4.8$ and by assuming $k_{\text{app}} < 1 \times 10^4 \text{ M}^{-1} \text{ s}^{-1}$ for the lower asymptote value (Figure 5). Hence, the upper asymptote value of $(6.2 \pm 0.2) \times 10^6 \text{ M}^{-1} \text{ s}^{-1}$ reflects the rate constant of HO_2^{\bullet} reaction with the deprotonated form of 3-carboxyproxyl. The apparent rate constants for the reaction of HO_2^{\bullet} with all five-membered ring nitroxides increased upon decreasing the pH below pH 2.7 (Table 3).

The second-order decay of superoxide was unaffected by the addition of 0.2–0.4 mM CHDO at pH 4.8 or pH 7.8 in the presence of 0.5 M PB, indicating that the rate constant of the

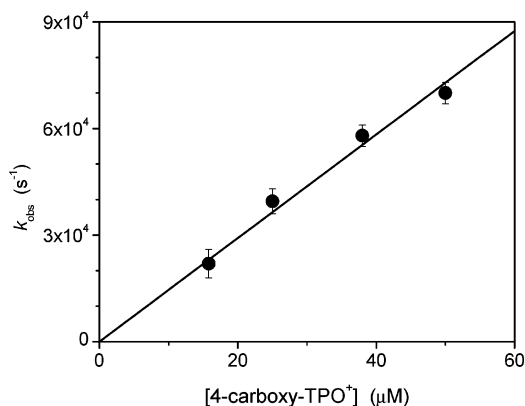


Figure 8. Reaction of 4-carboxy-TPO⁺ with O₂^{•−}. The decay of O₂^{•−} was followed upon pulse irradiation (13 Gy/pulse) of oxygenated solutions containing 4 mM PB at pH 8.1.

TABLE 3: Effect of pH on the Rate of HO₂[•] Reaction with Five-Membered Ring Nitroxides

nitroxide	pH	k _{app} (± 0.2), M ^{−1} s ^{−1}
3-aminomethylproxyl	3.6	1.0 × 10 ⁶
	2.8	1.2 × 10 ⁶
	2.1	2.1 × 10 ⁶
3-carboxyproxyl	2.7	2.0 × 10 ⁶
	2.0	4.0 × 10 ⁶
	1.3	1.2 × 10 ⁷
H-2954	3.6	1.9 × 10 ⁵
	2.8	3.4 × 10 ⁵
TCPO	3.6	1.9 × 10 ⁵
	2.8	3.4 × 10 ⁵
	2.1	1.3 × 10 ⁶
CHDO	1.46	7.0 × 10 ⁶
	3.6	1.4 × 10 ⁵
	2.9	1.8 × 10 ⁵
	2.6	3.2 × 10 ⁵
	2.3	4.0 × 10 ⁵
	1.9	1.0 × 10 ⁶
	1.5	4.0 × 10 ⁶
1.25	7.4 × 10 ⁶	

oxidation or reduction of CHDO by superoxide cannot exceed $5 \times 10^4 \text{ M}^{-1} \text{ s}^{-1}$, as is the case for all tested nitroxides.

Reaction of RN⁺=O with Superoxide. The reaction of O₂^{•−} with 4-carboxy-TPO⁺ was studied by pulse radiolysis of oxygenated solutions containing various concentrations of 4-carboxy-TPO⁺ at pH 8.1 (4 mM PB). Under such conditions e_{aq}[−] and H[•] are converted into O₂^{•−}, whereas [•]OH is scavenged by RN⁺=O. The effect of the latter reaction on the initial concentration of 4-carboxy-TPO⁺ at relatively low pulse intensity can be ignored, because its rate should be close to that of O₂^{•−} reaction with RN⁺=O. The decay rate of O₂^{•−} at 260–280 nm was linearly dependent on [4-carboxy-TPO⁺] (Figure 8), resulting in $k = (1.5 \pm 0.1) \times 10^9 \text{ M}^{-1} \text{ s}^{-1}$.

4-OH-TPO⁺ is relatively unstable,²⁸ and therefore, it was formed in situ via the reaction of [•]OH with 100 μM 4-OH-TPO in oxygenated solutions at pH 7.9 (4 mM PB). Under these conditions superoxide is being formed in excess over RN⁺=O, the latter being produced partly via the reaction of [•]OH with the nitroxide.²⁷ For comparison, this method has been previously applied for TPO⁺, and the corresponding rate constant has been determined under limiting concentrations of superoxide to be $(3.4 \pm 0.2) \times 10^9 \text{ M}^{-1} \text{ s}^{-1}$.²⁹ The decay rate of O₂^{•−} observed at 280 nm followed two subsequent first order reactions. The faster process was linearly dependent on [O₂^{•−}]_o, i.e., on the pulse intensity, resulting in $k = (3.4 \pm 0.2) \times 10^9 \text{ M}^{-1} \text{ s}^{-1}$ for both oxoammonium cations (Figure 9).

The slower first-order subsequent process was independent of the dose and was attributable to the decay of superoxide

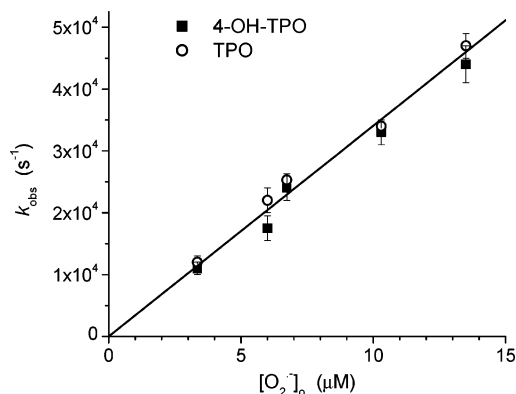


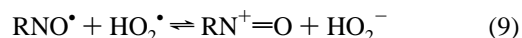
Figure 9. Reaction of 4-OH-TPO⁺ and TPO⁺ with O₂^{•−}. The decay of O₂^{•−} observed at 280 nm upon irradiation of oxygenated 4 mM PB solutions containing 100 μM 4-OH-TPO or TPO at pH 7.9 applying various pulse intensities.

radicals that have not been consumed by the initially formed RN⁺=O, but rather catalytically removed by the nitroxide. The determined rate constants of 1.5 ± 0.2 and $9.5 \pm 1.5 \text{ s}^{-1}$ for 4-OH-TPO and TPO, respectively, reflect the difference in their respective SOD-mimic activities.

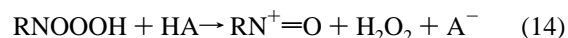
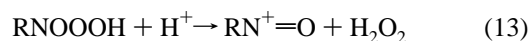
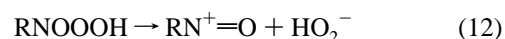
Discussion

The present study demonstrates that the reactivity of cyclic nitroxides toward [•]NO₂ and CO₃^{•−} radicals is independent of the ring-size and of the side chain (Table 2). The rate constant of the reaction of these nitroxides with [•]NO₂ is also pH-independent, and therefore, at physiological pH they are better scavengers than glutathione, cysteine or uric acid.⁵⁰ In contrast to [•]NO₂ and CO₃^{•−}, the reactivity of HO₂[•] toward cyclic nitroxides is highly dependent on the ring size and to a lesser extent on the side chain. All tested nitroxides react extremely slowly, if at all, with O₂^{•−}, whereas the latter reduces the various oxoammonium cations with a rate constant approaching the diffusion-controlled limit.

As previously suggested,²⁸ the reaction of the various nitroxides with superoxide takes place via reactions 9 and 10:



Using the Marcus equation, we have demonstrated²⁹ that the reaction of TPO and 3-carbamoylproxyl with HO₂[•] takes place via an inner-sphere electron-transfer mechanism and suggested that the decomposition of the adduct, RNOOOH, is likely to be both H⁺ and general acid catalyzed (the acids HA):



Under limiting concentrations of superoxide and at pH ≪ pK_a(HO₂[•]), the contribution of reaction 10 is negligible and rate eq 15 is obtained:

$$-\frac{d[\text{HO}_2^*]}{dt} = \frac{k_{11}(k_{12} + k_{13}[\text{H}^+] + k_{14}[\text{HA}])}{k_{-11} + k_{12} + k_{13}[\text{H}^+] + k_{14}[\text{HA}]} \times$$

$$[\text{RNO}^*]_0[\text{HO}_2^*] = k_{\text{app}}[\text{RNO}^*]_0[\text{HO}_2^*] \quad (15)$$

At pH > 4, reaction 10 becomes important and rate eq 16 is obtained where $[\text{O}_2^{*-}]_{\text{T}} = [\text{O}_2^{*-}] + [\text{HO}_2^*]$.

$$-\frac{d[\text{O}_2^{*-}]_{\text{T}}}{dt} = \frac{2k_{11}(k_{12} + k_{13}[\text{H}^+] + k_{14}[\text{HA}])}{k_{-11} + k_{12} + k_{13}[\text{H}^+] + k_{14}[\text{HA}]} \frac{[\text{H}^+]}{[\text{H}^+] + K_a} =$$

$$[\text{RNO}^*]_0[\text{O}_2^{*-}]_{\text{T}} = k_{\text{app}}[\text{RNO}^*]_0[\text{O}_2^{*-}]_{\text{T}} \quad (16)$$

Rate eqs 15 and 16 demonstrate the increase in k_{app} upon increasing the concentration of $[\text{H}^+]$ and/or $[\text{HA}]$, as shown in Figures 6 and 7. The value of k_{app} approaches a plateau value at high concentrations of $[\text{H}^+]$ and/or $[\text{HA}]$, where $k_{\text{app}}^{\text{max}} = k_{11}$ or $2k_{11}[\text{H}^+]/([\text{H}^+] + K_a)$. The $k_{\text{app}}^{\text{max}}$ values, obtained under different experimental conditions either by direct means or by plotting $1/k_{\text{app}}$ vs $1/[\text{PB}]_0$ or $1/[\text{formate}]_0$, and the calculated k_{11} values are summarized in Table 4.

For piperidine derivatives k_{11} is ca. $10^8 \text{ M}^{-1} \text{ s}^{-1}$, which is still rather high, although not diffusion-controlled, as we previously assumed.²⁹ For the five-membered ring compounds we observed H^+ catalysis but no buffer-induced catalysis, implying that the latter is too slow at feasible buffer concentrations. However, even the H^+ catalysis is rather inefficient and, therefore, we cannot determine k_{11} . In fact, we cannot even observe a pronounced downward curvature in the rate constants upon increasing $[\text{H}^+]$ (Table 3). This finding implies that either (i) an adduct is formed but, at feasible pH values the H^+ catalysis is too slow in comparison with the noncatalyzed decomposition or (ii) no adduct is formed on the reaction path and H^+ catalysis occurs by way of a third-order concerted reaction, where HO_2^* , the nitroxide and H^+ simultaneously form the transition state. If no adduct exists, the uncatalyzed reaction would have to be a one-step electron transfer. Such a reaction does not necessarily have to be an outer-sphere electron transfer, because, there being no steric or spin restrictions, the reactants can come quite close for substantial molecular overlap in the transition state to occur. If so, the rate constant may be significantly higher than that implied by the Marcus theory for an outer-sphere electron-transfer reaction.^{51,52}

Biological Implications. The well recognized toxic effects of reactive oxygen and nitrogen species in normal metabolism and under most pathophysiological processes partly result from the fast recombination of $\cdot\text{NO}$ and O_2^{*-} to yield ONOO^- .^{53–55} The latter reacts rapidly with CO_2 forming about 33% $\cdot\text{NO}_2$ and CO_3^{*-} ,⁵⁶ which under physiological conditions, where high concentrations of CO_2 prevail, are possibly the predominant peroxyxynitrite-derived cytotoxic species (Scheme 1). The search for more effective compounds, which diminish the damage caused by the various reactive species, includes SOD mimics and efficient scavengers of $\cdot\text{NO}_2$ or CO_3^{*-} to terminate radical chain reactions and restitute impaired cellular sites (Scheme 1).

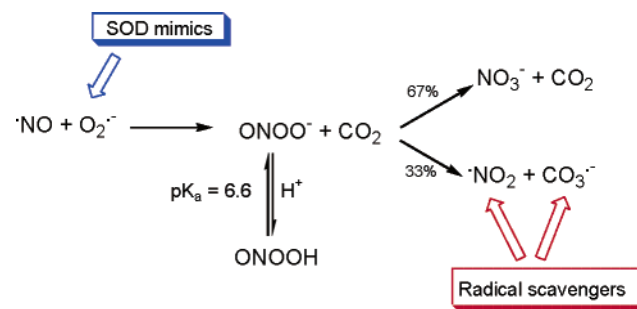
The present results show that piperidine, pyrrolidine and oxazolidine nitroxides are poor SOD mimics at physiological pH compared to native SOD. The best SOD mimics among the nitroxides are the six-membered ring derivatives, but even in the presence of high buffer concentration their catalytic activity is ca. 3 orders of magnitude lower than that of $\text{Cu}_2\text{Zn-SOD}$ at pH 7.4, i.e., $k_{\text{cat}} = 2k_{11}[\text{H}^+]/([\text{H}^+] + K_a) < 1 \times 10^6 \text{ M}^{-1} \text{ s}^{-1}$. It is worthwhile to note that at the pH range 4–5, which is

TABLE 4: k_{app} and the Derived k_{11} Values for Superoxide Reaction with the Six-Membered Ring Nitroxides

pH	[formate], M	[PB], M	$k_{\text{app}}^{\text{max}} (\pm 0.1), \text{M}^{-1} \text{ s}^{-1}$	$k_{11} (\pm 0.1), \text{M}^{-1} \text{ s}^{-1}$
4-amino-TPO ^a				
2.0–2.5	0.2	0	1.4×10^8	1.4×10^8
3.3	1.0	0	1.5×10^8	1.5×10^8
3.7	>1.0	0	1.4×10^8	1.5×10^8
4.8	5×10^{-3}	>0.1	1.3×10^8	1.3×10^8
6.7	5×10^{-3}	0.15	3.5×10^6	1.4×10^8
4-OH-TPO				
2.2–3.3	1.0	0	1.2×10^8	1.3×10^8
4.8	5×10^{-3}	>0.4	1.2×10^8 ^c	1.2×10^8
CAT-1				
3.0	>1.9	0	1.5×10^8	1.5×10^8
3.7	>1.0	0	1.3×10^8	1.4×10^8
4.8	5×10^{-3}	>0.6	1.3×10^8 ^c	1.2×10^8
4-oxo-TPO				
2.5	1.0	0	7.5×10^7	7.5×10^7
3.6	>1.0	0	7.1×10^7 ^e	7.6×10^7
4-carboxy-TPO ^b				
5.4	0.02	>0.3	3.5×10^7	1.8×10^8
<2.4	0.2		1.6×10^8 ^d	1.6×10^8
Tempene				
2.7	0.8	0	8.1×10^7	8.1×10^7
3.6	>0.3	0	7.3×10^7	7.8×10^7

^a $k_{\text{app}}^{\text{max}}$ at pH 2–6.7 is for the protonated form. ^b $k_{\text{app}}^{\text{max}}$ at pH 5.4 and at pH < 3 is for the deprotonated and the protonated forms, respectively. ^c Derived from extrapolation of the data in Figure 7. ^d Derived from eq 6 using the data at pH 3.0 and 2.4. ^e Derived from extrapolation of the data in Figure 6. ^f Calculated assuming that $k_{\text{app}}^{\text{max}}$ equals $k_{11}[\text{H}^+]/([\text{H}^+] + K_a)$ at pH < 3.7 and $2k_{11}[\text{H}^+]/([\text{H}^+] + K_a)$ at pH > 4, where $\text{p}K_a(\text{HO}_2^*) = 4.8$.

SCHEME 1: Formation and Decomposition of Peroxynitrite under Physiological Conditions and the Potential Sites of Intervention To Diminish Its Toxicity.



closer to that of biological membranes, their catalytic activity is about 1 order of magnitude lower than that of $\text{Cu}_2\text{Zn-SOD}$. The results also demonstrate that at physiological pH, nitroxides are the most efficient scavengers of $\cdot\text{NO}_2$ ($k = (3–9) \times 10^8 \text{ M}^{-1} \text{ s}^{-1}$) and among the most effective metal-independent scavengers of CO_3^{*-} radicals ($k = (2–6) \times 10^8 \text{ M}^{-1} \text{ s}^{-1}$). Our results do not indicate a correlation of the kinetics of nitroxides reactions with $\text{HO}_2^*/\text{O}_2^{*-}$, $\cdot\text{NO}_2$ and CO_3^{*-} radicals with their protective effect against biological damage. On the other hand, because the redox potential and the various rate constants for TCPO and H-2954 are almost identical, the difference between their biological effects is more likely attributable to H-2954 being a target-oriented nitroxide. A similar consideration applies also for 4-carboxy-TPO and 4-amino-TPO, which manifest similar chemical features but different biological effects.

Acknowledgment. This research was supported by grants from the US-Israel Binational Science Foundation (No. 2002013) and the Hungarian National Research Fund, OTKA T048334.

References and Notes

- (1) Fuchs, J.; Freisleben, H. J.; Podda, M.; Zimmer, G.; Milbradt, R.; Packer, L. *Free Radical Biol. Med.* **1993**, *15*, 415–423.
- (2) Gallez, B.; Bacic, G.; Goda, F.; Jiang, J. J.; Ohara, J. A.; Dunn, J. F.; Swartz, H. M. *Magn. Reson. Med.* **1996**, *35*, 97–106.
- (3) Lai, C. S.; Hopwood, L. E.; Swartz, H. M. *Exp. Cell Res.* **1980**, *130*, 437–442.
- (4) Morse, P. D. J.; Swartz, H. M. *Magn. Reson. Med.* **1985**, *2*, 114–127.
- (5) Froncisz, W.; Lai, C. S.; Hyde, J. S. *Proc. Natl. Acad. Sci. U.S.A.* **1985**, *82*, 411–415.
- (6) Swartz, H. M. *Free Radical Res. Commun.* **1990**, *9*, 399–405.
- (7) Brasch, R. C.; London, D. A.; Wesbey, G. E.; Tozer, T. N.; Nitecki, D. E.; Williams, R. D.; Doemeny, J.; Tuck, L. D.; Lallemand, D. P. *Radiology* **1983**, *147*, 773–779.
- (8) Pou, S.; Davis, P. L.; Wolf, G. L.; Rosen, G. M. *Free Radical Res.* **1993**, *23*, 353–364.
- (9) Kuppusamy, P.; Wang, P. H.; Zweier, J. L.; Krishna, M. C.; Mitchell, J. B.; Ma, L.; Trimble, C. E.; Hsia, C. J. C. *Biochemistry* **1996**, *35*, 7051–7057.
- (10) Mitchell, J. B.; Samuni, A.; Krishna, M. C.; DeGraff, W. G.; Ahn, M. S.; Samuni, U.; Russo, A. *Biochemistry* **1990**, *29*, 2802–2807.
- (11) Reddan, J. R.; Sevilla, M. D.; Giblin, F. J.; Padgaonkar, V.; Dziedzic, D. C.; Leverenz, V.; Misra, I. C.; Peters, J. L. *Exp. Eye Res.* **1993**, *56*, 543–554.
- (12) Howard, B. J.; Yatin, S.; Hensley, K.; Allen, K. L.; Kelly, J. P.; Carney, J.; Butterfield, D. A. *J. Neurochem.* **1996**, *67*, 2045–2050.
- (13) Cuzzocrea, S.; McDonald, M. C.; Mazzon, E.; Siritwardena, D.; Costantino, G.; Fulia, F.; Cucinotta, G.; Gitto, E.; Cordaro, S.; Barberi, I. *Brain Res.* **2000**, *875*, 96–106.
- (14) Miura, Y.; Utsumi, H.; Hamada, A. *Arch. Biochem. Biophys.* **1993**, *300*, 148–156.
- (15) Slater, A. F.; Nobel, C. S.; Maellaro, E.; Bustamante, J.; Kimland, M.; Orrenius, S. *Biochem. J.* **1995**, *306*, 771–778.
- (16) Patel, N. S. A.; Chatterjee, P. K.; Chatterjee, B. E.; Cuzzocrea, S.; Serrano, I.; Brown, P. A. J.; Stewart, K. N.; Mota-Filipe, H.; Thiemermann, C. *Free Radical Biol. Med.* **2002**, *33*, 1575–1589.
- (17) Zeltzer, G.; Berenshtein, E.; Kitrossky, N.; Chevion, M.; Samuni, A. *Free Radical Biol. Med.* **2002**, *32*, 912–919.
- (18) Hoffman, A.; Goldstein, S.; Samuni, A.; Borman, J. B.; Schwab, H. *Biochem. Pharmacol.* **2003**, *66*, 1279–1286.
- (19) Mitchell, J. B.; DeGraff, W.; Kaufman, D.; Krishna, M. C.; Samuni, A.; Finkelstein, E.; Ahn, M. S.; Hahn, S. M.; Gamson, J.; Russo, A. *Arch. Biochem. Biophys.* **1991**, *289*, 62–70.
- (20) Hahn, S. M.; Wilson, L.; Krishna, C. M.; Liebmann, J.; DeGraff, W.; Gamson, J.; Samuni, A.; Venzon, D.; Mitchell, J. B. *Radiat. Res.* **1992**, *132*, 87–93.
- (21) Bar-On, P.; Mohsen, M.; Zhang, R. L.; Feigin, E.; Chevion, M.; Samuni, A. *J. Am. Chem. Soc.* **1999**, *121*, 8070–8073.
- (22) Zhang, R. L.; Hirsch, O.; Mohsen, M.; Samuni, A. *Arch. Biochem. Biophys.* **1994**, *312*, 385–391.
- (23) Beckwith, A. L. J.; Bowry, V. W.; Ingold, K. U. *J. Am. Chem. Soc.* **1992**, *114*, 4983–4992.
- (24) Brede, O.; Beckert, D.; Windolph, C.; Gottinger, H. A. *J. Phys. Chem. A* **1998**, *102*, 1457–1464.
- (25) Cuzzocrea, S.; McDonald, M. C.; Mazzon, E.; Filipe, H. M.; Centorrino, T.; Lepore, V.; Terranova, M. L.; Ciccolo, A.; Caputi, A. P.; Thiemermann, C. *Crit. Care Med.* **2001**, *29*, 102–111.
- (26) Augusto, O.; Bonini, M. G.; Amanso, A. M.; Linares, E.; Santos, C. C. X.; De Menezes, S. L. *Free Radical Biol. Med.* **2002**, *32*, 841–859.
- (27) Samuni, A.; Goldstein, S.; Russo, A.; Mitchell, J. B.; Krishna, M. C.; Neta, P. *J. Am. Chem. Soc.* **2002**, *124*, 8719–8724.
- (28) Goldstein, S.; Samuni, A.; Russo, A. *J. Am. Chem. Soc.* **2003**, *125*, 8364–8370.
- (29) Goldstein, S.; Merenyi, G.; Russo, A.; Samuni, A. *J. Am. Chem. Soc.* **2003**, *125*, 789–795.
- (30) Goldstein, S.; Merenyi, G.; Samuni, A. *Chem. Res. Toxicol.* **2004**, *17*, 250–257.
- (31) Novak, I.; Harrison, L. J.; Kovac, B.; Pratt, L. M. *J. Org. Chem.* **2004**, *69*, 7628–7634.
- (32) Krishna, M. C.; Grahame, D. A.; Samuni, A.; Mitchell, J. B.; Russo, A. *Proc. Natl. Acad. Sci. U.S.A.* **1992**, *89*, 5537–5541.
- (33) Krishna, M. C.; DeGraff, W.; Hankovszky, O. H.; Sar, C. P.; Kalai, T.; Jeko, J.; Russo, A.; Mitchell, J. B.; Hideg, K. *J. Med. Chem.* **1998**, *41*, 3477–3492.
- (34) Shankar, R. A.; Hideg, K.; Zweier, J. L.; Kuppusamy, P. *J. Pharmacol. Exp. Ther.* **2000**, *292*, 838–845.
- (35) Dhanasekaran, A.; Kotamraju, S.; Karunakaran, C.; Kalivendi, S. V.; Thomas, S.; Joseph, J.; Kalyanaraman, B. *Free Radical Biol. Med.* **2005**, *39*, 567–583.
- (36) Hankovszky, H. O.; Hideg, K.; Bodi, I.; Frank, L. *J. Med. Chem.* **1986**, *29*, 1138–1152.
- (37) Hankovszky, O. H.; Sar, C. P.; Hideg, K.; Jerkovich, G. *Synthesis* **1991**, *1*, 91–97.
- (38) Buxton, G. V.; Stuart, C. R. *J. Chem. Soc., Faraday Trans.* **1995**, *91*, 279–281.
- (39) Kato, Y.; Shimizu, Y.; Lin, Y. J.; Unoura, K.; Utsumi, H.; Ogata, T. *Electrochim. Acta* **1995**, *40*, 2799–2802.
- (40) Israeli, A.; Patt, M.; Oron, M.; Samuni, A.; Kohen, R.; Goldstein, S. *Free Radical Biol. Med.* **2005**, *38*, 317–324.
- (41) Fuchs, J.; Nitschmann, W. H.; Packer, L.; Hankovszky, O. H.; Hideg, K. *Free Radical Res. Commun.* **1990**, *10*, 315–323.
- (42) Schwartz, R. N.; Peric, M.; Smith, S. A.; Bales, B. L. *J. Phys. Chem. B* **1997**, *101*, 8735–8739.
- (43) Saracino, G. A. A.; Tedeschi, A.; D'Errico, G.; Improta, R.; Franco, L.; Ruzzi, M.; Corvaia, C.; Barone, V. *J. Phys. Chem. A* **2002**, *106*, 10700–10706.
- (44) Baur, J. E.; Wang, S.; Brandt, M. C. *Anal. Chem.* **1996**, *68*, 3815–3821.
- (45) Fish, J. R.; Swartz, S. G.; Sevilla, M. D.; Malinski, T. *J. Phys. Chem.* **1988**, *92*, 3745–3751.
- (46) Morris, S.; Sosnovsky, B.; B., H.; Huber, C. O.; Rau, N. U. M.; Swartz, H. M. *J. Pharm. Sci.* **1991**, *80*, 149–152.
- (47) Fielden, E. M.; Roberts, P. B. *Int. J. Radiat. Biol.* **1971**, *20*, 355–362.
- (48) Mallard, W. G.; Ross, A. B.; Helman, W. P. *NIST Standard References Database 40, Version 3.0*, 1998.
- (49) Bielski, B. H. J.; Cabelli, D. E.; Arudi, R. L.; Ross, A. B. *J. Phys. Chem. Ref. Data* **1985**, *14*, 1041–1100.
- (50) Ford, E.; Hughes, M. N.; Wardman, P. *Free Radical Biol. Med.* **2002**, *32*, 1314–1323.
- (51) Ebersson, L.; Shaik, S. S. *J. Am. Chem. Soc.* **1990**, *112*, 4484–4489.
- (52) Merenyi, G.; Lind, J.; Shen, X.; Eriksen, T. T. *J. Phys. Chem.* **1990**, *94*, 748–752.
- (53) Beckman, J. S.; Beckman, T. W.; Chen, J.; Marshall, P. A.; Freeman, B. A. *Proc. Natl. Acad. Sci. U.S.A.* **1990**, *87*, 1620–1624.
- (54) Huie, R. E.; Padmaja, S. *Free Radical Res. Commun.* **1993**, *18*, 195–199.
- (55) Goldstein, S.; Czapski, G. *Free Radical Biol. Med.* **1995**, *19*, 505–510.
- (56) Goldstein, S.; Czapski, G. *J. Am. Chem. Soc.* **1998**, *120*, 3458–3463.